

Article

Heterogeneous Biocatalysts Prepared by Immuring Enzymatic Active Components inside Silica Xerogel and Nanocarbons-In-Silica Composites

Galina A. Kovalenko ^{1,2,*}, Larisa V. Perminova ¹, Anatoly B. Beklemishev ¹ and Valentin N. Parmon ^{1,2}

¹ Institute of Catalysis, 630090 Novosibirsk, Russia; perminova@catalysis.ru (L.V.P.); beklem@niibch.ru (A.B.B.); parmon@catalysis.ru (V.N.P.)

² Department of Chemistry, Novosibirsk State University, 630090 Novosibirsk, Russia

* Correspondence: galina@catalysis.ru; Tel.: +7-383-32-69-743

Received: 22 March 2018; Accepted: 20 April 2018; Published: 26 April 2018



Abstract: Proprietary results on preparation and studies of whole-cell and lysates-based heterogeneous biocatalysts with different enzymatic activity were reviewed. A peculiar method was developed for preparing these biocatalysts by immuring (entrapping) enzymatic active components (EAC) inside silica (SiO₂) xerogel and nanocarbons-in-silica composites. Properties of the multi-component composite biocatalysts such as enzymatic activity and operational stability were compared. The effect of the inclusion of nanocarbons such as nanotubes, nanofibers, and onion-like nanospheres with various texture, nanostructure and dispersion were thoroughly studied. With invertase-active biocatalysts, the direct correlation between an increase in the enzymatic activity of the nanocarbons-in-silica biocatalyst and efficiency of EAC adhesion on nanocarbons was observed. The steady-state invertase activity of the baker yeast lysates-based biocatalysts was determined to increase by a factor of 5–6 after inclusion of the multi-walled carbon nanotubes inside SiO₂-xerogel. With lipase-active biocatalysts, the effect of the included nanocarbons on the biocatalytic properties depended significantly on the reaction type. In interesterification of oil-fat blends, the biocatalysts without any included nanocarbons demonstrated the maximal lipase activity. In esterification of fatty acids with aliphatic alcohols, the activity of the biocatalysts increased by a factor of 1.5–2 after inclusion of the aggregated multi-walled carbon nanotubes (CNTs) inside SiO₂-xerogel. In the low-temperature synthesis of isopentyl esters of butyric (C4:0), capric (C10:0), and stearic (C18:0) fatty acids, the lipase-active composite CNTs-in-silica biocatalysts operated without loss of activity for more than thousand hours.

Keywords: heterogeneous biocatalysts; immuring enzymatic active components; nanocarbons-in-silica composite

1. Introduction

Biocatalysis is of great practical importance and used for deliberate conversion of the one target substrate (S) into a commercially important valuable product (P) through a single enzymatic reaction, with the high chemo-, regio- and enantio-selectivity. Biocatalysis is an interdisciplinary field of knowledge; and many disciplines are needed for its successful implementation: enzymology and biochemistry; molecular biology and gene engineering; industrial microbiology; kinetics and catalysis; transport phenomena (diffusion kinetics); engineering and design of high-capacity reactors. Areas of application of biocatalysis are mainly the food and pharmaceutical industry, less the manufacture of fine and basic chemicals. More than hundred industrial-scale biocatalytic processes using enzymes or whole non-growing microorganisms, of more than 100 kg capacities were described elsewhere [1–5]. Biocatalytic

processes penetrated the large-tonnage food industry, including the production of glucose-fructose syrups and interesterified oil-fat blends.

Heterogeneous biocatalysts prepared by immobilizing enzymatic active substances such as enzymes or whole microorganisms are in the heart of modern biotech processes of “green” chemistry. The main advantage of the immobilization is a combination of the activity and unique selectivity of enzymes, as well as enhancement of their operational stability with the heterogeneity of the biocatalysts applied in the continuous or periodic bioprocesses.

Heterogeneous biocatalytical processes are considered more commercially attractive for large-scale implementation than homogeneous technologies due to considerable simplification and reduction (1.2–1.4 times) of the total production cost. In order to reduce the cost of the heterogeneous biocatalysts and the contribution of this cost into the final product, not purified enzymes isolated from microbial strain-producers but the whole non-growing microbial cells, as well as partially or fully disrupted microorganisms (lysates or sonicates) can be used. Such approach allows the multi-stage enzyme purification to be avoided; this is especially labor- and time-consuming process if the enzyme is intracellular and not extracted during bacteria growth in the nutrient media. In most cases, whole-cell or lysates-based biocatalyst are highly active and stable, probably, due to more friendly environment in the vicinity of native enzyme. The drawback is the relatively low specific enzymatic activity normalized to 1 mg of dry-weight substances; in some cases, it is 1–2 orders of magnitude lower than that per 1 mg of immobilized purified enzyme. However, in majority cases there may take place diffusion limitations to mass transfer of the substrate toward individual enzyme immobilized usually on mesoporous supports, and no more than 10–20% of activity of soluble enzyme is determined after immobilization. Meanwhile, the enzymatic activity of whole or fully disrupted microorganisms is almost completely retained after immobilization; and the whole-cell and lysates-based biocatalysts operate in the kinetic (not diffusion) regime. Therefore, despite significant differences in the initial enzymatic activity, the final activities of the biocatalysts prepared by immobilization of either enzymes or whole microorganisms are of the same order. Indeed, the commercial biocatalyst for glucose isomerization prepared using the purified glucose isomerase are only 2–3 times more active than the biocatalysts prepared using substantially less active (by orders of magnitude) whole *Streptomyces* sp. cells [3].

Inorganic silica-based supports often are used for immobilization of enzymatic active substances; and some commercially available heterogeneous biocatalysts are prepared using silica or silicates. For example, the glucose isomerase-active biocatalyst Optisweet® is prepared by cross-linking of *S. rubiginosus* adsorbed on the commercial silica. Another example is the lipase-active biocatalyst Lipozyme® TL IM prepared by immobilization of recombinant *Thermomyces lanuginosus* lipase on aerosil. Silica-based supports may be divided into the following groups: (i) commercial granulated mesoporous silica and glasses; (ii) natural minerals—clay, diatomite, zeolites; and (iii) modern silica material synthesized using various silanes and sol-gel techniques. Many recent scientific publications are devoted to encapsulation (entrapment) of enzymes into synthetic silica-based supports (iii) [6].

Obviously, the inorganic supports are selected for the heterogeneous biocatalyst preparation due to their availability and relatively low cost as well as high mechanical strength and durability of biocatalysts granules in the reaction media. The main role is to improve noticeably the operating parameters both of down-stream processes using the traditional continuous packed-bed reactors and periodic processes using the batch stirred-tank reactors [7]. Novel types of reactors—a rotor inertial reactor and an immersed vortex reactor, were specially designed for the heterogeneous biocatalysts in order to enhance of the process productivity [8,9].

Immobilization by adsorption/adhesion of enzymatic active substances on inorganic supports has a high commercial potential but some enzymes and microorganisms are poorly fixed on solid surfaces because of their natural peculiarities. For example, *Arthrobacter nicotianae* cells producing glucose isomerase did not adhere on the surfaces of the majority of macroporous inorganic supports such as foam-like ceramics, foamed carbon, vermiculite, corundum, CNFs- or coke-coated minerals; the observed adhesion was less than 0.1 mg of dry-weight cells per 1 g of adsorbent [10]. The maximal

adhesion of *A. nicotianae*, 1.6 mg/g, was observed on the *Sapropel* type macroporous carbon-mineral supports [11]. Thus, the immobilization by adhesion of whole non-growing *A. nicotianae* cells is not suitable for preparing GI-active biocatalysts. Thus, research and development of a universal, simple and inexpensive method of immobilization of various enzymatic active substances, including microorganisms of different taxonomy, was in demand. Entrapping (or immuring, or embedding) inside silica-based matrices seemed the most appropriate and attractive method for preparing highly active and stable heterogeneous biocatalysts. A peculiar universal method of immobilization was first developed for the non-adhered *A. nicotianae* cells and described in papers published in 2009–2010 [12–14].

In this authors' report, the results on study of multi-component heterogeneous biocatalysts prepared by immuring enzymatic active substances inside silica xerogel and nanocarbons-in-silica composites were summarized. Whole non-growing microorganisms, as well as fully disrupted bacteria and yeast cells (named lysates) were used as an active component for preparing biocatalysts with the desired enzyme activity. Advanced carbonic materials such as nanotubes, nanofibers, and nanospheres were examined for inclusion inside SiO₂-based biocatalysts. The properties of whole-cell and lysates-based heterogeneous biocatalysts such as enzymatic activity and operational stability, were systematically and thoroughly investigated as dependent on their compositions, in particular on texture and nanostructure of the nanocarbons included. Multi-component composition of the biocatalysts was optimized individually for the each enzymatic active substance and type of reaction. Biocatalysts with the highest activity and stability were investigated in the corresponding biotransformation processes such as hydrolysis, isomerization, interesterification and esterification.

2. Results and Discussion

2.1. Procedure for Immuring Enzymatic Active Substances Inside Silica Xerogel and Nanocarbons-In-Silica Composites

A peculiar method of preparing whole-cell biocatalysts was first developed for the non-adhered *A. nicotianae* cells in 2008–2009, as mentioned above. The main stages were following: (I) thorough mixing of all components including EAC with silica hydrogel; (II) drying of the mixture; (III) crushing of the dried mixture and fractionation to 0.4–4 mm sized granules of biocatalysts.

Stage I—mixing. Silica hydrogel was prepared by the sol-gel method via slow precipitation of sodium silicate (liquid glass, Na₂SiO₃) with ammonium nitrate at pH 7.5 and 70 °C; the precipitation rate was 300 g (SiO₂)·L^{−1}·h^{−1} [15]. The precipitated SiO₂-hydrogel was washed to neutral pH, pressed and squeezed, then stored as a gelatinous mass in a dense polyethylene bag for several years. The SiO₂-hydrogel humidity was 80–90%. Microbial biomass as EAC for preparing whole-cell biocatalysts was the non-growing microorganisms such as *A. nicotianae*, baker yeast *Saccharomyces cerevisiae* and recombinant *E. coli* strains producing glucose isomerase or lipase. Biomass as EAC for preparing lysates-based biocatalysts was fully disrupted cells of *S. cerevisiae* and recombinant *E. coli* strain via enzymatic lysis. The biomass humidity was 75–95%. Additional functional components such as activator of enzyme, or moisture-holder, or nanocarbons, were mixed with SiO₂-hydrogel in order to improve properties of the final biocatalysts. In the case of GI-active biocatalysts, insoluble cobalt(II) hydroxides were included in order to increase the stability of the biocatalysts. In the case of LIP-active biocatalysts, the maltodextrin was added to prevent quick dehydration of the biocatalysts during operation in anhydrous reaction media. Carbonic material such as nanotubes, nanofibers, onion-like nanospheres, or nanodiamonds were added into SiO₂-hydrogel for possible additional binding EAC by adsorption/adhesion on nanocarbons to decrease their leakage into reaction media and enhance operational stability of the biocatalysts.

Stage II—drying. After stage I, drying of the wet multi-component biocatalyst in a stationary thin bed under ambient conditions (room temperature, air humidity 40–60%) for 1–3 days was carried out. The humidity of dried biocatalysts was 5–15%. Variations in the drying conditions, for example in flowing dry nitrogen at 20–40 °C, did not affect the properties of the biocatalysts. During drying silica hydrogel transformed into SiO₂-xerogel with specific surface area of 200–250 m²/g.

Stage III—granulation. In the case of GI-active biocatalysts operated in aqueous buffer media, pH 7–8, and at elevated temperature, 60–70 °C, the mixture dried at stage II was pre-ground into a fine powder, then compressed at 50–150 bar and, finally, fractionated for obtaining solid granules 1–4 mm in size suitable for filling into a packed bed reactor. In the case of LIP-active biocatalysts operated in anhydrous reaction media of oil-fat blends or organic solvents, the mixture dried at stage II was carefully mechanically crushed and fractionated as granules 1–2 mm in size.

Accomplishment and finish of I–III stages resulted in the preparation of the multi-component heterogeneous biocatalysts. One can see from the above description that the developed method of immobilization of various EAC was simple in implementation, did not require expensive equipment and aggressive reagents (e.g., silanes). Toxic pollutants and corrosive wastewater was not formed. This method was universal with respect to taxonomy of microorganisms and the chemical nature of the functional components added to the silica hydrogel at stage I. The general regularities for the biocatalysts granules with high mechanical strength were as follows: (1) the content of silica as the main binder was no less than 20%; (2) the content of the nanocarbons was no more than 15%.

2.2. Selection of the Optimal Compositions of the Biocatalysts

Properties of the prepared multi-component biocatalysts depending on the ratio of all components in SiO₂-xerogel were thoroughly studied. The biocatalysts' composition was optimized by the simultaneous satisfaction of two parameters, namely, (1) the maximal enzymatic activity; and (2) high stability of granules due to its mechanical strength and durability in the reaction media. Durability of the biocatalysts' granules in the aqueous media was estimated visually. For instance, after several hours of periodic operation in hydrolysis, the not optimized whole-cell biocatalysts were converted into an amorphous formless mass; the granules were destroyed. Such simultaneous satisfaction ensured the high operational stability of the biocatalysts in continuous and periodic processes, and, as a result, the high productivity. Optimal compositions of the whole-cell biocatalysts are shown in Table 1. Referring to this Table, the optimal content of microbial biomass depended upon the taxonomy of microorganisms. For example, the optimal contents of *A. nictotianae* and *rE. coli/xyl* biomass inside GI-active biocatalysts were 10–15 w/w % and 35–40 w/w %, respectively (Table 1).

Table 1. Optimal compositions of the whole-cell biocatalysts prepared by immuring non-growing microorganisms inside silica xerogel and nanocarbons-in-silica composites.

Microorganism	Biocatalytical Process	Optimal Composition, wt %				
		Microbial Biomass	Co _x O _y	Maltodextrin	Carbon Nanotubes	SiO ₂
<i>S. cerevisiae</i>	Sucrose inversion	60–80	0	0	5–10	20–30
<i>A. nictotianae</i>	Glucose/fructose	10–15	20–40	0	0	45–70
<i>rE. coli/xyl</i>	isomerization	35–40	10–40	0	0–5	20–40
<i>rE. coli/lip</i>	Tributylin hydrolysis	35–40	0	0	5–10	50–55
	Interesterification	35–40	0	10–20	0	40–55

The optimal content of included nanocarbons (carbon nanotubes) depended both on the taxonomy of microorganisms and on the type of the enzymatic reaction (Table 1). For example, the properties of GI-active biocatalysts depended slightly upon the presence of included nanocarbons because of weak adhesion of *A. nictotianae* cells as mentioned above. The activity of LIP-active whole-cells biocatalysts in hydrolysis of triglyceride was twice as high when the CNTs were included [16]. On the other hand, in interesterification the activity of nanocarbons-free (without included CNTs) biocatalysts was maximal [17]. It was of interest to elucidate the function of nanocarbons included into the composite biocatalysts. It was first assumed that the main role of nanocarbons was to hold enzymatic active substances inside biocatalysts due to adsorption/adhesion in order to ensure high biocatalytic activity and stability as mentioned above. Indeed, the direct proportion between the adhesion of yeast autolysates and steady-state invertase activity of the biocatalysts was found [18]. The further study of LIP-active composite biocatalysts revealed that hydrophobic substrates such as triglycerides were

adsorbed tightly onto highly hydrophobic nanocarbons and, as a result, essential water was displaced from the vicinity of immobilized lipase; and the activity of the composite biocatalysts decreased. Thus, different functional roles are characteristic of included nanocarbons.

3. Texture of the Biocatalysts

The texture of the whole-cell biocatalysts was studied. The specific surface area ($S_{sp,BET}$) depended both on the taxonomy of the microorganisms and on the composition of the multi-component biocatalysts (Table 2). When the content of the microbial biomass was less than 15 w/w %, the specific surface area of the biocatalysts was 250 m²/g that was close to $S_{sp,BET}$ of the parent SiO₂-xerogel (without biomass), 260 m²/g. When the content of the baker yeast biomass increased up to 80 w/w %, the surface area of these biocatalysts decreased from 250 to 35 m²/g (Table 2).

Table 2. Textural characteristics of the whole-cell biocatalysts depending on taxonomy of immobilized microorganisms and composition of the prepared multi-component biocatalysts.

Microorganism	Biocatalyst Composition, w/w % of Dry Substances				$S_{sp,BET}$, m ² /g	V , cm ³ /g	D_{pore} , nm
	Biomass	SiO ₂	CoSO ₄	Co _x O _y			
<i>S. cerevisiae</i>	15	85			250	0.6	22
	20	80			220	0.9	15
	60	40			100	0.6	22
	80	20			35	0.4	36
<i>A. nictotianae</i>	15	85	0.06		230	0.9	15
	10	50		40	175	0.6	13
<i>rE. coli/xyl</i>	40	40		20	75	0.35	19
<i>rE. coli/lip</i>	40	60			90	0.6	25

The porosity of the dried biocatalysts was studied mainly by Hg-intrusion method; and pore size distribution curves were analyzed. Mesopores with diameter 2–50 nm were estimated to occupy more than 50–80% of the total pore volume (V_{Σ}), and macropores with diameter more than 50 nm less than 20% of V_{Σ} . The absence of micropores smaller than 2–3 nm was indicated by N₂ porosimetry as well. In the whole-cell biocatalysts with low biomass content (10–15 w/w %), the pore distribution was similar to the pure mesoporous SiO₂-xerogel. It was found that the higher content of baker yeast biomass, the wider distribution of pore sizes and the larger average diameter of pores (Table 2, Figure 1a). SEM-images in Figure 1a (right) demonstrated that macropores could be formed by “shadow” defects of the dried cells entrapped inside SiO₂-xerogel. Almost identical pore size distribution was observed for the glucose isomerase-active biocatalysts prepared by entrapment of *A. nictotianae* and *rE. coli/xyl* cells (Figure 1b). Thus, mesoporous texture was characteristic of the whole-cell biocatalysts (Table 2, Figure 1).

Mesoporous textures were characteristic of the lysate-based biocatalysts as well. Comparative consideration of Figures 1 and 2 led to conclusions about predomination of mesopores, but neither macropores nor micropores are in the pore structure of both biocatalysts. The mesopore diameter distribution was wider in the *rE. coli/lip* lysate-based than in yeast lysates-based biocatalysts (Figure 2). The average pore diameter of the former was about two times as large as that of the latter (Table 3).

The texture of the composite nanocarbons-in-silica biocatalysts was also examined. $S_{sp,BET}$ of the composite lysate-based biocatalysts decreased by a factor of 1.1–1.8 against that of the biocatalysts without nanocarbons (Table 3). For example, after inclusion CNT1s inside yeast autolysate-based biocatalysts $S_{sp,BET}$ decreased insignificantly, whereas pore volume and average diameter increased as follows: V_{Σ} from 0.3 to 0.5 cm³/g, D_{pore} from 11 to 19 nm. It was shown that the higher specific surface area of included nanocarbon, the greater specific surface area of the composite biocatalyst (Table 3). Hence, the mesoporous texture was characteristic of the lysates-based biocatalysts and their nanocarbons-in-silica composites (Table 3, Figure 2).

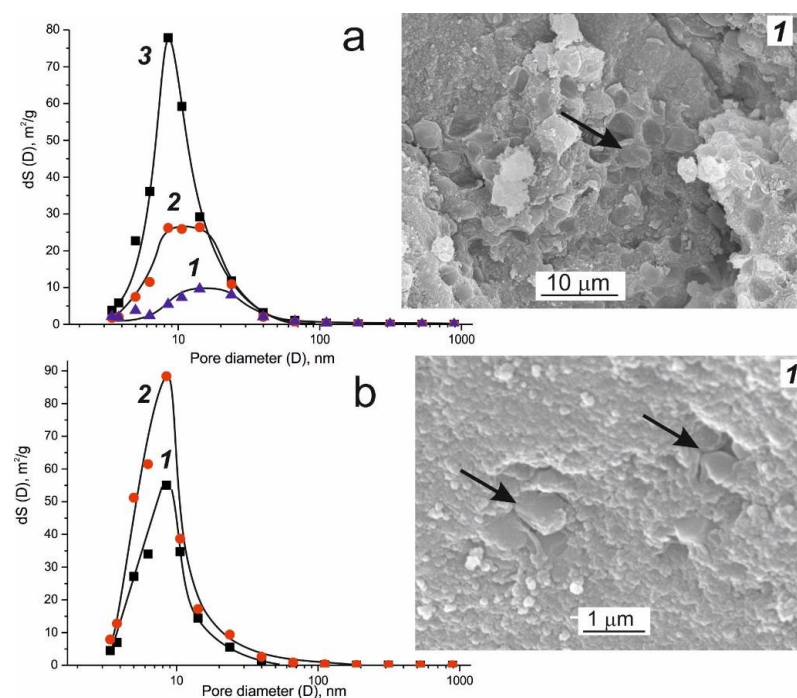


Figure 1. (Left) Pore size distributions: (a) entrapped *S. cerevisiae* biomass in contents of 20 w/w % (1), 60 w/w % (2) and 80 w/w % (3); (b) entrapped *A. nictotianae* (1) and *rE. coli/xyl* (2) biomass in content of 15 w/w %. (Right) SEM images of cleavages of the whole-cell biocatalysts. Arrows indicate microbial whole cells entrapped inside SiO_2 -xerogel.

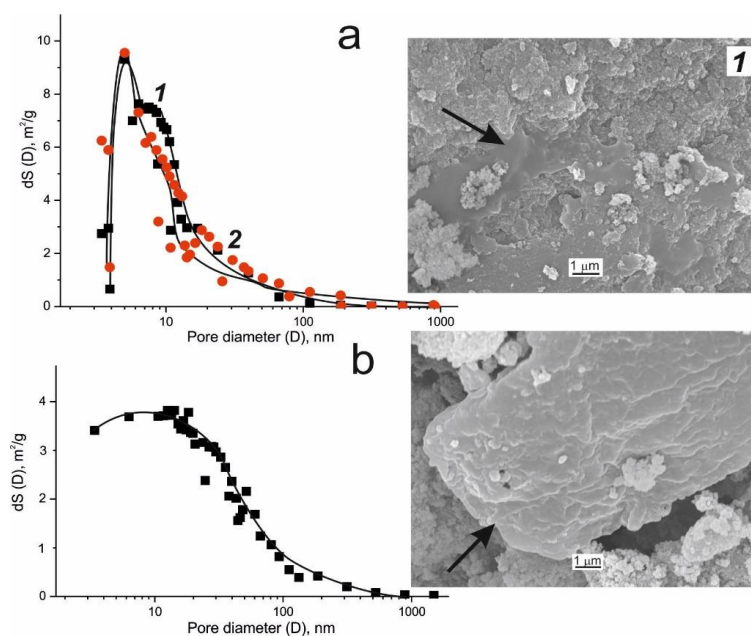


Figure 2. (Left) Pore size distribution: (a) baker yeast autolysates entrapped inside SiO_2 -xerogel without nanocarbon (1, \blacksquare) and with CNT1s (2, \bullet), (b) *rE. coli*/lip lysates entrapped inside SiO_2 -xerogel without nanocarbon. (Right) SEM images of cleavages of the lysate-based biocatalysts. Arrows indicate the smooth area corresponding to lysates entrapped in SiO_2 -xerogel.

Table 3. Textural characteristic of composite lysate-based biocatalysts depending on the type of included nanocarbons and enzymatic activity of prepared biocatalyst.

Type of Included Nanocarbon * ($S_{sp.BET}$ of Nanocarbons)	Baker Yeast Autolysate-Based Biocatalysts		rE. coli/lip Lysate-Based Biocatalysts	
	$S_{sp.BET}$, m^2/g	D_{pore} , nm	$S_{sp.BET}$, m^2/g	D_{pore} , nm
Without nanocarbons	110	11	105	31
Carbon nanotubes CNT1 ($320 m^2/g$)	105	19	90	25
Carbon nanofibers CNF ($160 m^2/g$)	60	12		
Carbon nanospheres CNS1 ($485 m^2/g$)	95	11	110	22
Nanodiamond ND ($325 m^2/g$)	80	14		

* Content of nanocarbons inside biocatalysts was 15 w/w %.

The results obtained lead to conclude about mesoporous texture of all the prepared biocatalysts. Particular attention was paid to the macrokinetics of biocatalytic heterogeneous processes under study. The conditions for biocatalyst operation in the kinetic (not diffusion) regime were chosen experimentally. The mesoporous texture of the biocatalysts makes the mass transfer of substrates toward entrapped enzymatic active component free of internal diffusion limitations [12,13,18,19].

The single-enzymatic activity and operational stability of the prepared multi-component biocatalysts and their properties for the process of substrate conversion into valuable product are discussed below.

4. Heterogeneous Whole-Cell and Lysates-Based Biocatalysts

4.1. Glucose Isomerase-Active Biocatalyst

The whole-cell biocatalysts were prepared by immuring native *A. nicotianae* and recombinant rE. coli/xyl non-growing bacteria cells producing thermostable glucose isomerase intracellularly. The high thermostability of microbial GI provided a linear increase in the enzymatic activity of the biocatalysts with temperature (T) in the range of 55 to 85 °C with the T-coefficient equal to 1.3–1.5; the inactivation half-life time ($t_{1/2}$) of the biocatalysts heated at 80 °C in the buffer solution, pH 7.8, was equal to 6–7 h [12].

As mentioned above, the optimization of composition of the GI-active biocatalyst has to provide the highest enzymatic activity along with the high mechanical strength and durability of the granules during operation in buffer, pH 7–8, at 60–75 °C in a flow packed-bed reactor. Referring to Table 1, the optimal content of *A. nicotianae* biomass varied only in a relatively narrow range from 10 to 15 w/w %. When the biomass content was more than 15 w/w %, the mechanical strength of the biocatalyst fell down quickly; and the granules were destructed and transformed into an amorphous paste within 1–2 h of the operation.

It is of common knowledge that Mg(II) and Co(II) ions activate glucose isomerase and enhance the stability of this enzyme. Various Co(II)-containing component were included into whole-cell biocatalysts. With a soluble Co(II) component, e.g., $CoSO_4$, the biocatalysts' granules had relatively low durability, and the half-life times ($t_{1/2}$) of the biocatalysts were no longer than 20–24 h in buffer at 75 °C. Therefore, insoluble Co(II) compounds were studied as a functional component of the GI-active biocatalysts. Freshly prepared Co(II) hydroxide was precipitated by adding gradually ammonia solution (NH_4OH) to cobalt nitrate ($Co(NO_3)_2$). The intensely blue colored precipitate identified as unstable $\beta-Co(OH)_2$ was dried and transformed to grey-green $Co_3O_4 \cdot nH_2O$ and then to $CoO/Co_3O_4(Co_xO_y)$. Granules of the dried biocatalysts containing insoluble Co_xO_y turned color from grey-green to pink during operation under the reaction conditions (pH 7.8, 70–75 °C). The pink color indicated predomination of stable cobalt hydroxide $\alpha-Co(OH)_2$ species inside the biocatalysts. Inclusion of insoluble Co_xO_y (not soluble $CoSO_4$) resulted in 1.5–1.6 times increase in the glucose isomerase activity of the biocatalysts, as well as in an increase in durability of the granules in the

reaction medium and, therefore, in enhancement of the operational stability under studied conditions. The optimal content of Co_xO_y was 20–40 w/v % (Table 2); the composition of GI-active whole-cell biocatalysts was covered by a patent [20].

The commercial technology of glucose isomerization (but not the process using the prepared here biocatalysts containing insoluble Co_xO_y) needs addition of Co^{2+} ions (1 mM) to the glucose solution. We analyzed the samples of the produced glucose-fructose syrup at the outlet of packed-bed reactor to show that the Co and Si concentrations in the product (syrup) were practically constant during 816 h operation at 65 ± 5 °C and equal to $1\text{--}2 \mu\text{g}\cdot\text{mL}^{-1}$ (max. 0.03 mM Co^{2+}) and $16\text{--}36 \mu\text{g}\cdot\text{mL}^{-1}$, respectively. Thus, the usage of the prepared GI-active biocatalyst for monosaccharide isomerization allowed us to decrease the Co^{2+} concentration in the final product by a factor of 30–70.

The glucose isomerase activity of the biocatalysts prepared by immuring recombinant strain-producer *rE. coli/xyl* was ten times as high as that for entrapped *A. nictotianae* ($100\text{--}500 \text{ U}\cdot\text{g}^{-1}$ vs. $10\text{--}30 \text{ U}\cdot\text{g}^{-1}$) [21]. Referring to Figure 3, the stability of the *rE. coli/xyl* whole-cell biocatalysts was two-fold higher than for entrapped *A. nictotianae*; the half-life time was found to be more than 1200 h under studied conditions [13,21].

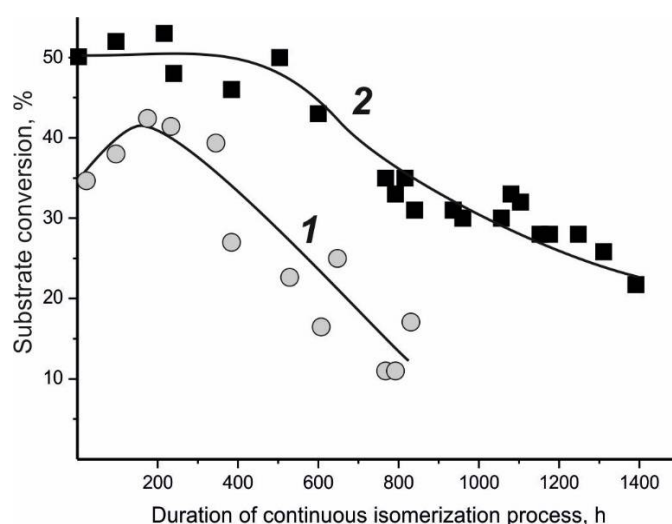


Figure 3. Dependence of substrate conversion at the outlet of column packed-bed reactor on the duration of continuous isomerization of fructose by the *A. nictotianae* (1) and *rE. coli/xyl* (2) whole-cell biocatalyst. Reaction conditions: 65 °C, 3 M fructose, 0.02 M phosphate buffer pH 7.8 and 7.0 for *A. nictotianae* and *rE. coli/xyl* respectively, 1 mM Mg^{2+} . Contact time was 5.5 h.

The composite nanocarbons-in-silica whole-cell biocatalysts were prepared using *rE. coli/xyl* cells, Co_xO_y component and various types of nanocarbons such as CNTs, CNFs, CNSs and nanodiamond. The bulk morphology of these biocatalysts was examined with a scanning electron microscope (Figure 4).

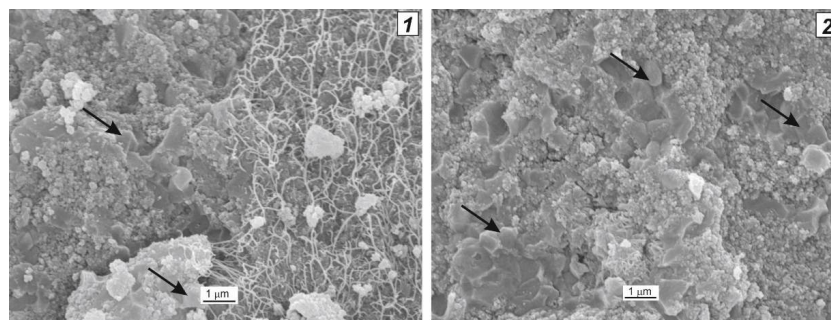


Figure 4. SEM images of cleavages of the whole-cell biocatalysts prepared by immuring *rE. coli*/xyl cells inside SiO₂-xerogel with included CNTs (1) and CNFs (2). Arrows indicate entrapped bacteria.

An inconsiderable effect of inclusions of nanocarbons on the activity and stability of the GI-active biocatalysts was observed and described in [18]. The steady-state glucose isomerase activity was $\sim 100 \text{ U} \cdot \text{g}^{-1}$ for the biocatalysts except nanocarbons-containing composite biocatalysts which were only 10–15% more active. The main reason was found to be the weak adsorption/adhesion of GI-active substances on nanocarbons and leakage of enzymatic active component from biocatalysts [18]. The dried biocatalysts were cross-linked with glutaric dialdehyde (less than 1 v/v%); the steady-state activity increased by a factor 1.5 in comparison with the non-crosslinked biocatalysts, and the enhanced stability was determined. These biocatalysts retained fully their initial activity during 28 periodic reaction cycles under the reaction conditions (pH 7.0, 70 °C) [18].

4.2. Invertase-Active Biocatalyst

Analysis of the literature showed that more than a quarter of studies on immobilization of non-growing *S. cerevisiae* (baker yeast) cells were devoted to only single, namely invertase activity for hydrolysis of disaccharide (sucrose) to equimolar mixture of monosaccharides (glucose and fructose), the so-called invert syrup. The invert syrup as a sweetener is valuable and marketable product of food industry. A majority of INV-active heterogeneous biocatalysts were prepared by immobilization of whole cells of baker yeast [22–26]; the yeast autolysates and purified intracellular invertase as an EAC were described rarely. For example, the baker yeasts were immobilized by adhesion to a composite material, jute fabric coated by polyethyleneimine; and this biocatalyst operated in a column reactor without loss in efficiency to hydrolyze concentrated (60–80%) sucrose syrups for 45 days at 45 °C [22]. The most active and stable biocatalyst described in literature [24] was prepared by mutual bonding of native baker yeasts with polyethyleneimine and glutaraldehyde. The specific invertase activity of this biocatalyst was $300\text{--}1500 \text{ U} \cdot \text{g}^{-1}$; the half-life of the biocatalyst was 500–1000 h (pH 4.6, 60–75 °C). The total biocatalyst productivity over the period of its lifetime was 2–10 tons of hydrolyzed sucrose per 1 kg of the biocatalyst [24].

Silica gel was first described for encapsulation (inclusion) of *S. cerevisiae* cells into thin SiO₂-layers deposited on glass sheets [26]. The precursors of silica gel were various silanes (not liquid glass, as described here); the hydrolysis and polycondensation of silanes occurred after addition of aqueous solution of enzymatic active substances. In most cases silanes and products of their hydrolysis were toxic reagents and inhibited enzymes. For example, the specific invertase activity was 3.6 times decreased after inclusion of *S. cerevisiae* cells into SiO₂-gel formed during polycondensation of tetra-ethoxysilane [26].

In this report, neutral and inert SiO₂-xerogel obtained without any toxic reagents was found to be friendlier matrix for preparing highly active biocatalysts; the invertase activity reached $500\text{--}700 \text{ U} \cdot \text{g}^{-1}$ that was comparable in magnitude with the best results described in [24]. It was found that the INV activity of the whole-cell biocatalysts depended linearly on the baker yeast content from 5 to 80 w/w %. Exactly, due to high content of non-growing *S. cerevisiae* cells inside biocatalysts their activities were

high. The process of sucrose inversion was carried out both in periodic and continuous mode in stirred-tank and packed-bed reactors respectively. The full conversion of 50 *w/v* % sucrose into invert syrup was reached for less than 7 h at 50 °C; the biocatalyst operated without loss of activity during 25–30 reaction cycles. In the continuous process of sucrose inversion, the half-life time of the whole-cell biocatalyst was more than 200 h (pH 4.6, 50 °C) [27].

Yeast autolysates are fully disrupted cells via lysis by own intracellular enzymes such as lysozyme, and this EAC were used for preparing invertase-active biocatalysts. Earlier the biocatalysts were prepared by adhesion of baker yeast autolysates on natural materials such as expanded clay, Saprorels, and lignin [28]. It was found that macroporous Saprorels were the most efficient supports for adhesion of yeast autolysates, but the steady-state activity of such biocatalysts was comparatively small (avg. 60 U·g^{−1}) [11,28]. Here, the baker yeast autolysates were used as an active component of the biocatalysts prepared by immuring inside silica xerogel and nanocarbons-in-silica composites. It was shown that the invertase activity of these lysate-based biocatalysts was 2–3 times higher than for the whole-cells biocatalysts with similar compositions. The interior morphology of the composite nanocarbons-in-silica lysate-based biocatalysts examined with a scanning electron microscope is shown in Figure 5.

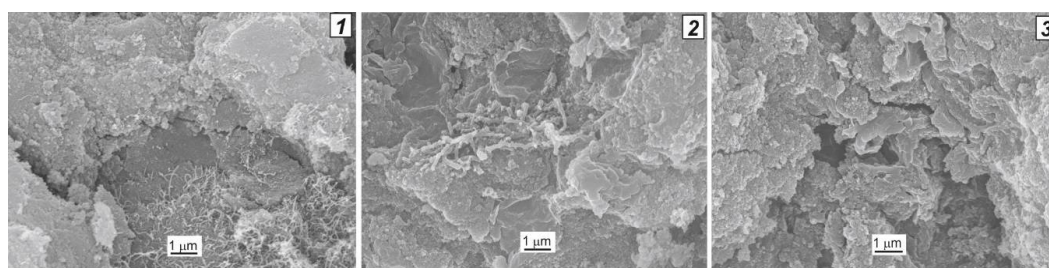


Figure 5. SEM images of cleavages of the biocatalysts prepared by immuring baker yeast autolysates inside nanocarbons-in-silica composites: 1—CNTs, 2—CNFs, 3—CNSs. Smooth areas corresponded to entrapped autolysates.

Pronounced positive effect on the properties of autolysate-based biocatalyst was observed with all types of nanocarbon included inside SiO₂-xerogel (Figure 6); the maximal steady-state invertase activity was more than 3000 U·g^{−1} (vs. 60 U·g^{−1} for adhered autolysates). A correlation between adhesion ability of yeast autolysates on nanocarbons and properties of composite biocatalysts was found: the more efficient adhesion of autolysates, the higher was steady-state activity [18]. For example, an increase in the content of included CNFs up to five-fold (from 5% to 25%) provided an increase in the steady-state activity of the biocatalysts by a factor of 1.8. The values of tight adhesion of yeast autolysates on CNTs and CNFs were determined as 5 and 2 mg/g respectively. As one can see in Figure 6, the steady-state activities of composite biocatalysts such as CNTs-in-silica and CNFs-in-silica were proportional to their capability of adhering autolysates. The values of steady-state activities of composite lysate-based biocatalysts were 2–6 times higher than that of nanocarbons-free biocatalysts based on SiO₂-xerogel (Figure 6). With the composite biocatalysts, *t*_{1/2} in continuous sucrose inversion process was 200–500 h (pH 4.6, 50 °C).

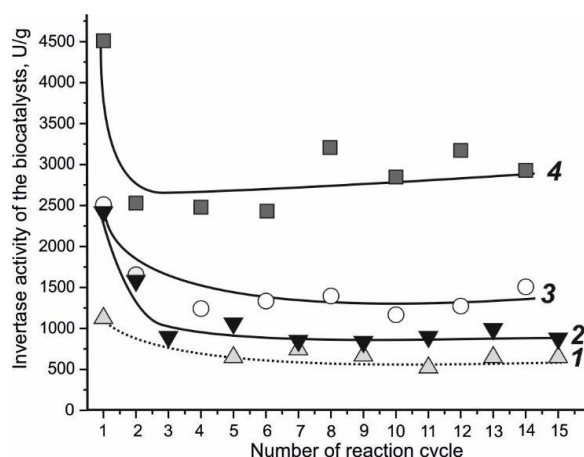


Figure 6. The invertase activity of lysate-based biocatalyst in dependence of type of nanocarbon included and numbers of reaction cycles of sucrose inversion: 1—without nanocarbon (dotted line), 2—CNFs, 3—CNS1s, 4—CNT1s. Reaction conditions: 50 °C, 2 M sucrose, 0.02 M acetate buffer pH 4.6.

4.3. Lipase-Active Biocatalyst

Much attention is given now to the application of lipases in industry. Microbial lipases are a powerful tool for catalytic hydrolytic breakdown of fats and oils followed by the formation of free fatty acids, diglycerides, monoglycerides, and glycerol. The reverse synthetic reactions such as esterification, acidolysis, alcoholysis, and aminolysis of fatty acids, as well as triglyceride interesterification are of most interest [1–5]. The development of the commercially attractive inexpensive, highly active and stable heterogeneous biocatalysts is still an exciting goal. A number of reviews [29–35] deal with methods for immobilization of lipases, as well as properties of the prepared lipase-active biocatalysts, such as enzyme activity, stability, regio- and enantio-selectivity.

Extracellular production of lipases is characteristic of a majority of native microorganisms but recombinant *E. coli* strains usually synthesize lipase intracellularly. The authoring constructed *rE. coli*/lip strain was found to produce recombinant *T.lanuginosus* lipase in the amount of ~30–40% of the total cell protein [36]. The study of recombinant lipase localization inside *rE. coli*/lip cells showed that more than 70% of the lipase activity was localized in the intracellular cytoplasm, and only small values of activity in debris and inclusion bodies [36]. The specific lipase activity of suspended *rE. coli*/lip whole cells was rather low (2.5 U per 1 mg of dry substances). Partial disruption of cells via drying and thawing led to ~20-fold increase in the observed activity (45 U·mg^{−1}), whereas the full disruption of cells via enzymatic lysis and sonification increased the lipase activity by two orders of magnitude (210 U·mg^{−1}) [19,36].

The partially disrupted *rE. coli*/lip cells, and *rE. coli*/lip lysates, and recombinant His₆×lipase purified by affinity chromatography were studied as EAC for preparing lipase-active heterogeneous biocatalysts based on SiO₂-xerogel and nanocarbon-in-silica composites. Interior morphology of the composite lysate-based biocatalysts was examined with electron-scanning microscope (Figure 7).

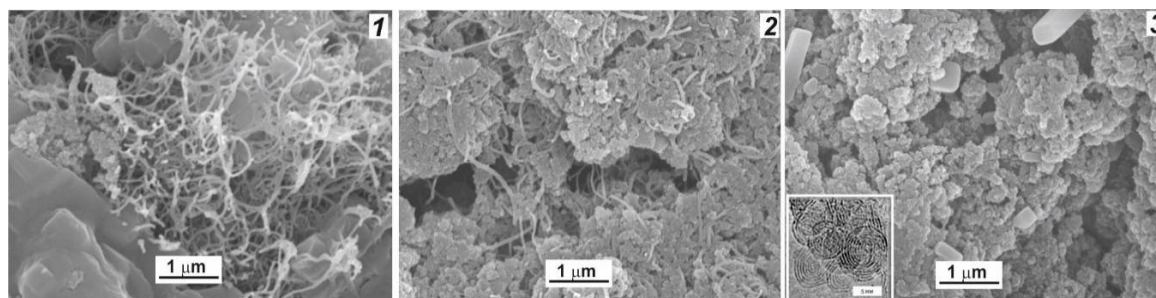


Figure 7. SEM images of cleavages of the biocatalysts prepared by immuring *rE. coli*/lip lysates inside nanocarbons-in-silica composites: 1—CNT1s, 2—CNT2s, 3—CNSs. Smooth areas correspond to entrapped lysates. The nanostructure of CNSs (in insert 3) was examined with high-resolution transmission microscope.

The lysate-based biocatalysts were found to be the most active, they being 4–8 and 2–16 times more active than the whole-cell biocatalysts and the immobilized recombinant lipase, respectively (Table 4). Referring to this Table, the hydrolytic activity decreased to one fifth upon supersonic dispersion of 100–150 μm nanocarbon aggregates into separate primary nanotubes distributed more uniformly inside SiO_2 -xerogel. This phenomenon was described elsewhere [16]. In addition, the reasons for decrease in activity of immobilized lipase associated with peculiarities of lipase molecular structure and high hydrophobicity of nanocarbons were discussed. As illustrated in the scheme [16], the active site of adsorbed lipase may be blocked by hydrophobic surface of nanotubes or nanospheres; the apparent inactivation of the biocatalysts was observed, especially pronounced for uniformly distributed nanotubes. The important role of mutual correspondence of the hydrophobic-hydrophilic natures of immobilized enzyme and immobilizing support was discussed firstly in 1988 [37] and confirmed in previous [38,39] and current studies. As a result of tuning properties of inorganic supports including surface morphology toward immobilizing enzymes (alcohol dehydrogenase, glucoamylase and invertase), it was found that the synthesis of CNFs on the surface of the aluminosilicate honeycomb monolith and ceramic foam allowed preparing the highly active and stable biocatalysts due to mesoporous texture and optimal hydrophilic-hydrophobic properties of the surface carbons [39].

Table 4. Hydrolytic activities (in $\text{U} \cdot \text{g}^{-1}$) of prepared lipase-active biocatalysts depending on the origin of enzymatic active component and nanocarbons included inside silica xerogel.

Type of Nanocarbon Included in Content of 10 w/v %	Enzymatic Active Component		
	Partially Disrupted <i>rE. coli</i> /lip Cells	Lysates of <i>rE. coli</i> /lip Cells	His ₆ × Lipase Purified *
Without nanocarbons	210	870	510
Multi-walled CNT1 (5–11 nm in diameter) <i>aggregated</i>	220	1050	120
Multi-walled CNT1 (5–11 nm in diameter) <i>dispergated</i>	50	400	25
Multi-walled CNT2 (20–22 nm in diameter) <i>aggregated</i>	250	870	260
Carbon onion-like nanospheres (5–6 nm in diameter) <i>aggregated</i>	105	710	

* Recombinant lipase was purified by affinity chromatography on Ni-NTA Sepharose.

Below is authors' report of the most effective *rE. coli*/lip lysate-based biocatalysts prepared and studied in the following reactions: (1) hydrolysis of tributyrin [16,19]; (2) interesterification of oil-fat blends [16,19,36,40]; (3) interesterification of sun flower oil with ethyl acetate [40,41]; (4) esterification of fatty acid with aliphatic alcohols [36,42]. It was found that the rates of reactions were considerably in more than 500 times higher in aqueous buffered media (hydrolysis) than in anhydrous organic solvents

(esterification). However, low-temperature enzymatic synthesis of esters is of more importance as an alternative to organic synthesis of these valuable products to be applied in perfume and cosmetic industries as odorants, emollients, and inert surfactants.

The effect of inclusion of nanocarbons into lysate-based LIP-active biocatalysts depended on the type of catalyzed reaction. The rates of reactions with participation/formation of water (hydrolysis/esterification, respectively) were maximal when *rE. coli*/lip lysates were entrapped inside CNTs-in-silica composites (Table 5). The rates of reactions with triglycerides (interesterification in anhydrous media) were maximal when *rE. coli*/lip lysates were entrapped inside nanocarbons-free SiO₂-xerogel (Table 5).

Table 5. Relative activity * of *rE. coli*/lip lysate-based biocatalysts in various reactions.

Type of Aggregated Nanocarbon Included **	The Type of Reaction (Reaction Media)			
	Hydrolysis of Emulsified Tributyrin (Aqueous)	Interesterification in Oil-Fat Blends (Anhydrous)	Interesterification of Oil with Ethyl Acetate (in Hexane)	Esterification of Capric Acid with Isopentanol (in Hexane with Diethyl Ether)
Without nanocarbons	0.9	1.0	1.0	0.3
CNT1	1.0	0.9	0.8	
CNT2	0.8	0.9	1.0	1.0
CNS1	0.7	0.5	0.4	
CNS2	0.9		0.8	0.5

* The maximum activity was taken as 1.0; ** content of nanocarbons inside biocatalysts was 10 w/w %.

Operational stability of the lipase-active biocatalysts also depended on the type of catalyzed reaction. In periodic interesterification of oil-fat blends in a stirred-tank reactor, the stability of all lysates-based biocatalysts was low enough; the half-life time was no longer than 10–15 h at 70 °C [19]. In continuous/periodic interesterification of oil-fat blends in a lab-scale packed-bed reactor, the stability of the lysates-based biocatalysts was higher at the half-life time longer than 70 h at 70–75 °C (Figure 8a). In periodic interesterification of sunflower or linseed oils with methyl- or ethyl acetate in a stirred-tank reactor, the stability of the biocatalysts was even higher at the half-life time longer than 600–700 h at 40 °C (Figure 8b). Generally, the highest operational stability of the composite biocatalysts was observed when aggregated CNT2s (but not dispersed CNTs and CNSs) were used for the biocatalyst preparation (Figure 8b).

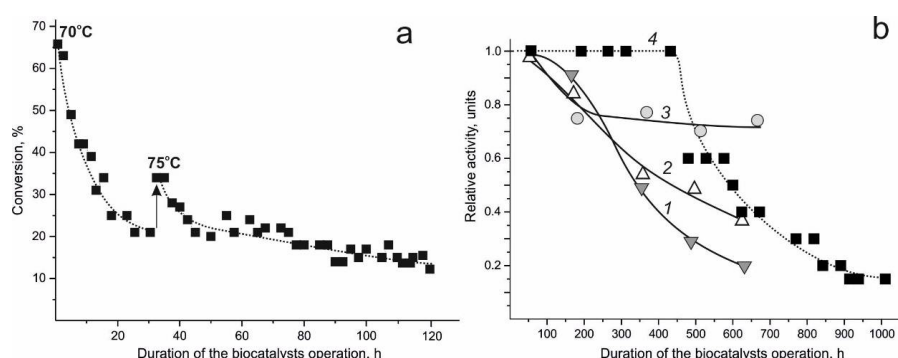


Figure 8. Operational stability of *rE. coli*/lip lysate-based biocatalysts in the processes: (a) Continuous/periodic interesterification of oil-fat blends at 70–75 °C; the biocatalyst composition, in w/w %: *rE. coli*/lip lysate—37–38, maltodextrin—10, SiO₂—till 100. (b) Periodic interesterification of sunflower oils with ethyl acetate at 40 °C; the biocatalyst composition, in w/w %: *rE. coli*/lip lysate—25–28, maltodextrin—10, nanocarbons—10, 1—CNSs, 2—CNT1s, 3—CNT2s, 4—without nanocarbon (dotted line), SiO₂—till 100.

One of the reasons for inactivation of the lipase-active biocatalysts during long-term interesterification in anhydrous media was the dehydration of biocatalysts because of replacement

of essential water from the vicinity of immobilized lipase by highly hydrophobic substrate—oil triglycerides. In periodic esterification of fatty acids with isopentanol, the stability of all prepared biocatalysts was extremely high; the biocatalysts operated without the activity loss longer than several hundred hours at 40 °C [36,42] due to accumulation of essential water as a product of this reaction inside biocatalysts.

The study of selectivity of the lipase-active heterogeneous biocatalysts in esterification toward the structure of substrates—acid and alcohol—was started by the authors; the initial results were described in [36,43]. The rate of esterification was higher for fatty acids with 10 and 18 carbon atoms in the molecule than for butyric acid with 4 carbon atoms (Figure 9), whereas cyclic and aromatic acids reacted at the lowest rates close to zero. Inclusion of carbon nanotubes provided the two-fold increase in activity of the biocatalysts and some changes of selectivity (Figure 9). The systematic study on selective esterification by immobilized recombinant lipase is in progress now, and possible modulation of the selectivity via biocatalysts engineering is of great interest.

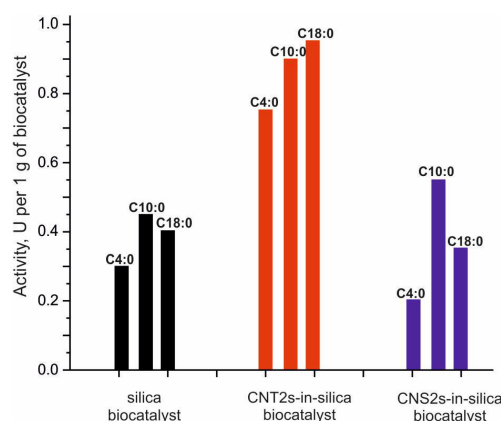


Figure 9. Activity of *rE. coli*/lip lysate-based biocatalysts and the nanocarbons-in-silica composites in reaction of esterification of fatty acids such as butyric C4:0, capric C10:0 and stearic C18:0 with isopentanol. Reaction conditions: 20 °C, 0.1 M fatty acid, 0.2 M isopentanol, hexane and diethyl ether in ratio 1:1. Reactions were performed in six replicates.

5. Materials and Methods

5.1. Enzymatic Active Substances

5.1.1. Glucose Isomerase Active Component of the Biocatalysts

Bacteria strains producing glucose isomerase such as *Arthrobacter nicotianae* deposited in the collection of non-pathogenic microorganisms and recombinant strain-producer *E. coli* BL21(DE3)/pET24bxylA (designated as *rE. coli*/xyl) were provided by colleagues from the Institute of Microbiology (Minsk, Belarus) and described in a number of papers [12,13,20,21]. *A. nicotianae* biomass was harvested by centrifugation at 10,000 g for 15 min. The *rE. coli*/xyl biomass was collected at the end of the late logarithmic phase or at the beginning of the steady-state phase by centrifugation at 5000 rpm for 15 min. The humidity of the biomass was 75–80 w/w %.

The specific activities of *A. nicotianae* cells in buffered suspension, pH 7.8 were avg. 150 and 550 U·per 1 g of dry cells at 60 and 75 °C, respectively. The glucose isomerase activity in *rE. coli*/xyl cell suspension was avg. 3000 U per 1 g of dry cells at 70 °C.

The glucose isomerase activity were measured in the medium of 0.02 M phosphate buffer pH 7.0 (for *rE. coli*/xyl) and 7.8 (for *A. nicotianae*) at 60–75 °C. Fructose in concentration of 2–3 M was used as a substrate. In order to determine the enzymatic activity in cell suspensions, ions of Mg²⁺ and Co²⁺ as 1 mM sulfate salt solutions were added to the reaction medium. No Co²⁺ ions were added to the reaction medium for measuring the activity of heterogeneous biocatalysts containing insoluble Co_xO_y.

The concentration of glucose produced via fructose isomerization was determined using HPLC [13] and spectrophotometric techniques with glucose oxidase (GO) as a selective reagent for glucose, for example, using procedure described in [44] with GO, KJ and NaMoO₄.

5.1.2. Invertase Active Component of the Biocatalysts

Commercial *Saccharomyces cerevisiae* baker yeasts was suspended in 0.02 M acetate buffer pH 4.6 and used for preparing whole-cell biocatalysts. The invertase activity in cell suspension was avg. 6000 U per 1 g of dry cells at 50 °C.

Yeast autolysates were obtained by autolysis of commercial baker yeast under continuous stirring at 50 ± 1 °C for 18–22 h. The autolyzed biomass was collected by centrifugation at 5000 rpm for 30 min, the supernatant was withdrawn, and the sediment was then re-suspended in 0.15 M KCl and washed. This procedure was three or four times repeated until the supernatant became transparent and colorless. The beige-colored paste-like sediment of yeast autolysates contained 20–22 w/w % of dry substances (the humidity was 78–80 w/w %) was used for biocatalysts preparation.

The invertase activity was measured in 0.02 M acetate buffer pH 4.6 at 50 °C using 0.6 M sucrose as a substrate. The analysis of glucose as a product of sucrose inversion was done with glucose oxidase [44]. The invertase activity in suspension was avg. 30,000 U per 1 g of dry autolysates at 50 °C.

5.1.3. Lipase Active Component of the Biocatalysts

The recombinant *E. coli* BL21(DE3) strain producing thermostable lipase (denoted as r*E. coli*/lip) was constructed by cloning chemically synthesized gene of mature *Thermomyces lanuginosus* lipase in the pJExpress 401 expression vector under the control of the bacteriophage T5 promoter as described in [16,19,36]. When the cultivation of the recombinant strain-producer was completed, the r*E. coli*/lip biomass was harvested by centrifugation at 3000 g for 20 min. The sediment was re-suspended in 10 mM phosphate-buffered saline pH 8.0. The lipase activity was measured in the reaction of hydrolysis of 0.2 M tributyrin in 0.02 M phosphate buffer pH 7.0 at 20 °C. Glycerol (1.2 M) and Gum arabic (0.6 w/v %) were added to reaction medium for emulsifying tributyrin. The lipase activity of suspended r*E. coli*/lip cells was avg. 50 U per 1 g of dry cells.

Lysates of r*E. coli*/lip cells were obtained as follows. The harvested recombinant cells were suspended and incubated with 1–2 mg·mL^{−1} lysozyme in ice for 30 min, then sonicated in an ultrasonic disintegrator at the maximum power of 300 W for 20–30 s. Then, MgCl₂, DNAase and RNAase A solutions were added to sonicated cells at the final concentrations of 5 mM, 10 µg·mL^{−1} and 50 µg·mL^{−1}, respectively. This mixture was placed in a water bath and incubated at 20 °C for 10 min, then sonicated again seven times for 15–20 s in ice in the ultrasonic disintegrator at the maximum power. The suspension of twice sonicated cells was centrifuged, and the supernatant (named r*E. coli*/lip lysates) was collected and used for preparation of LIP-active biocatalysts. The hydrolytic lipase activity of r*E. coli*/lip lysates in suspension was avg. 150 U per 1 g of dry lysates.

The relative experimental error of measuring enzymatic activity was no more than 15%.

5.2. Silica Hydrogel and Nanocarbon Materials

Silica hydrogel was obtained via coagel formation in continuous sol–gel procedure using sodium silicate (liquid glass, Na₂SiO₃) reacting with ammonium nitrate at pH 7.5 and 70 °C [15]. The hydrogel humidity was 80–90 w/w %. Drying of silica hydrogel at 105–120 °C resulted in the formation of mesoporous silica xerogel (SiO₂–xerogel) with the specific surface area (S_{sp.BET}) equal to 260 m²/g, total pore volume (V_Σ) 0.5–0.6 cm³/g and average pore diameter (D_{pore}) 20–22 nm.

Fine powders of nanostructured carbons were used for preparing multi-component composite biocatalysts. Texture characteristic of the nanocarbons are listed in Table 6. Multi-walled carbon nanotubes (CNTs) were synthesized by CVD ethylene decomposition over supported Fe,Co-catalyst at 670 °C [45]. Carbon nanospheres with onion-like structure (CNSs) were synthesized by high temperature annealing of nanodiamonds in vacuum at 1600 °C [46,47]. Nanodiamonds (NDs) of

4–6 nm in size were produced in Biysk, Russia and contained 85–91 *w/w* % of carbon. The primary particles of CNTs, CNSs and NDs were associated to 100–200 nm aggregates; these aggregates were dispersed using an ultrasonic disintegrator as follows. The aggregated nanocarbons, in particular CNTs, were mixed with SiO₂-hydrogel and distilled water, then treated with ultrasound at 22 kHz-frequency and 300W power for 30 min in a water-cooled vessel.

Table 6. Texture characteristic of nanocarbons.

Type of Nanocarbon	Diameter of Primary Particle, nm	S _{sp,BET} , m ² /g
CNT1	9–11	320
CNT2	20–22	140
CNF	20–60	160
CNS1	5–6	485
CNS2	8–10	250
ND	4–6	325

Carbon nanofibers (CNFs) with the “fishbone” structure were synthesized by methane pyrolysis over supported Ni-catalysts [48,49]. Bulk CNFs granules were grinded to fine powder in a mortar prior to the preparation of biocatalysts.

5.3. Biocatalytic Processes of Substrate Conversion

5.3.1. Substrates and Reagents

Tributyrin and butyric acid were purchased from MP Biomedicals, LLC. Gum Arabic was purchased from Fluka. Sucrose, fructose and vegetable oils such as sunflower and linseed oils were purchased in a local food-shop. Hexane, diethyl ether, methyl and ethyl acetate, isopentanol, glycerol, and organic acids including saturated fatty acids (capric C10:0 and stearic C18:0) were produced in Russia. All the reagents and solvents used were of analytical grade.

5.3.2. Monosaccharide (Glucose, Fructose) Isomerization

The continuous process of isomerization of monosaccharides (glucose and fructose) was carried out in a plug flow packed-bed reactor. The reactor was filled with the prepared GI-active biocatalyst granules of 1–4 mm in size and inert filler, such as glass balls of 2 mm in diameter, their volume ratio being 1:1. The use of the filler reduced significantly the pressure drop of the bed. The reactor was placed into a thermostat at 65 ± 5 °C, and 3 M monosaccharide solution was run through the bed downward at the flow rate of 0.02 mL·min^{−1}. Aliquots were taken at the reactor outlet in regular intervals (once per day) and glucose concentrations were analyzed. The conversion (in %) of the substrate was calculated, and half-life time ($t_{1/2}$) was determined.

5.3.3. Sucrose Inversion

The activity of the invertase-active biocatalysts was measured using a circulation set-up consisting of a differential gradientless column reactor with a thin bed of the prepared biocatalyst (0.1–0.5 g). The thermostat was maintained at given temperature (50–60 °C) of the reaction medium and in the biocatalyst bed. A peristaltic pump provided circulation of the substrate solution through the biocatalyst bed at the flow rate 1–35 mL·min^{−1}. The duration of one reaction cycle ranged from 2 to 8 h. After finishing the reaction cycle, the reaction medium was removed, and the biocatalyst was rinsed with distilled water and buffer. The steady-state activity of the biocatalyst was determined after conditioning biocatalysts as described elsewhere [18].

5.3.4. Interesterification of Oil-Fat Blends

The interesterification of oil-fat blend was carried out in periodic mode in a stirred-tank reactor and in a lab-scale set-up comprising a flow packed-bed bioreactor at 60–75 °C [16,17]. Initial blends and interesterified (final) products were analyzed using a pulsed NMR spectrometer. The conversion (x , %) was calculated from the decrease in the solid fat content measured at 35 °C in final products in comparison with initial oil-fat blends. The initial blends were prepared by mixing vegetable (soybean, sunflower or oleic) oils with heated fully hydrogenated one in proportion of 2–3 parts of oil to 1 part of hydrogenate. The interesterification in the lab-scale set-up was performed as follows. A stainless still column reactor was filled with 0.5–2 mm granules of the *rE. coli*/lip lysate-based biocatalyst of mixing uniformly with the inert filler such as 1–2 mm granules of commercial silica at the volume ratio of 3:1. Samples for analysis were collected every 3 h. The temperature in the reservoir with substrate and in reactor was kept at 70–75 °C. Initial oil-fat blends were pumped through the fixed bed at the flow rate of 0.12 mL·min^{−1} for 8–10 h. Then the flow of blends was stopped and the reactor was cooled down to 20–22 °C. After 14–15 h storage, the next reaction cycle was started by heating the reservoir and the reactor up to 70–75 °C. The biocatalyst was tested in this regime for 120 h.

5.3.5. Interesterification of Vegetable Oil with Ethyl Acetate

The interesterification of vegetable oil with methyl- or ethyl acetate was carried out in periodic mode in a stirred-tank reactor on a shaker at 120–150 rpm and 40 °C. The reaction medium had the following composition: 0.1 M oil, 2.3–2.5 M ethyl acetate, solvent—*n*-hexane. Depending on the activity of the prepared biocatalyst, the duration of one reaction cycle ranged from 5 to 144 h. The products—ethyl esters of fatty acids—were analyzed using gas (GC) and thin-layer chromatography (TLC) under the conditions described elsewhere [41].

5.3.6. Esterification of Fatty Acids with Aliphatic Alcohols

Esterification was carried out in periodic mode in a stirred-tank reactor on a shaker at 70 rpm and 40 °C. Two substrates (S) used for esterification were following: substrate S_1 —butyric C4:0, capric C10:0, and stearic C18:0 fatty acids, as well as benzoic and phenoxyacetic acids; substrate S_2 —isoamyl alcohol (isopentanol). The reaction medium had the following composition: 0.1 M acid (S_1) and 0.2 M alcohol (S_2) in solvent—mixture of hexane and diethyl ether in a 1:1 ratio. The duration of one reaction cycle was 24 h. The esterification rate was determined from the consumption of the organic acid involved in the synthesis of the ester. The concentration of S_1 was determined titrimetrically with water-ethanol solution of NaOH with known concentration. The conversion (x , in %) of the S_1 was calculated.

6. Main Equipment

The texture parameters of the heterogeneous biocatalysts were examined by both the nitrogen adsorption/desorption and mercury intrusion porosimetry using ASAP 2400 V3.07 and AUTO-PORE IV 9500 V1.09 devices (Micromeritics Instrument Corporation, Norcross, GA, USA), respectively. The specific surface areas ($S_{sp.BET}$) were measured by thermal desorption of argon using a SORBI-M instrument (ZAO Meta, Novosibirsk, Russia). The content of nanocarbons was determined gravimetrically and by thermal analysis using a STA-449 C Jupiter instrument (Netzsch, Selb, Germany). The morphology of the cleavages of the biocatalysts was examined with a scanning electron microscope (SEM) JSM 6460 LV (JEOL Ltd., Tokyo, Japan). Marks in the SEM images corresponded to the distance in μ m. A pulsed NMR spectrophotometer (ZAO Chromatek, Yoshkar-Ola, Russia) was used for measuring the solid fat contents in oil-fat blends and interesterified products.

7. Conclusions

Multi-component heterogeneous biocatalysts were prepared using a peculiar method developed for immobilization both of whole non-growing microorganisms and fully disrupted microbial cells (lysates) by immuring inside silica xerogel and nanocarbons-in-silica composites. Properties of these whole-cell and lysate-based biocatalysts such as single-enzymatic activity and operational stability were investigated systematically. The effect of the included nanocarbons such as nanotubes, nanofibers, onion-like nanospheres on the activity and stability of composite biocatalysts was studied.

With glucose isomerase-active whole-cell biocatalysts, only inconsiderable effect after inclusion of nanocarbons on the properties of the composite nanocarbons-in-silica biocatalysts was established. The glucose isomerase activity was only 1.1–1.15 times as high as that of the nanocarbons-free SiO₂-xerogel because of weak adhesion of *A. nicotianae* and recombinant *rE. coli/xyl* bacteria on nanocarbons. The cross-linking of the dried biocatalysts by 0.1–1% glutaric dialdehyde led to increase in one and half times biocatalytic activity; the maximal steady-state activity was 160 U·g^{−1} at 70 °C. The operational stability was enhanced as well; $t_{1/2} > 1200$ h under continuous glucose/fructose isomerization.

With invertase-active biocatalysts, there was significant positive effect after inclusion of nanocarbons inside silica xerogel. The maximal effect on properties of the composite lysate-based biocatalysts was observed upon inclusion of CNTs, the invertase activity being as high as 2–6 times of that of the nanocarbons-free biocatalysts. The highest steady-state activity, 3000 U·g^{−1} at 50 °C, was determined for the composite CNTs-in-silica lysate-based biocatalysts; $t_{1/2} > 200$ h under continuous sucrose inversion at 50 °C. Correlation between the adhesion ability of yeast lysates on nanocarbons and the steady-state activity of the biocatalysts was found.

The lipase-active biocatalysts prepared by immuring *rE. coli/lip* lysates inside silica xerogel and nanocarbons-in-silica composites, the effect of the included nanocarbons on biocatalytic activity and stability depended significantly on the reaction type. In interesterification of oil-fat blends, the biocatalysts prepared without nanocarbons and with inclusion of maltodextrin demonstrated the highest activity and stability. The half-life time was ~70 h at 70–75 °C. In interesterification of sunflower oil with ethyl acetate, the most active and stable biocatalysts were prepared both without nanocarbons and with included CNT2s. The half-life time was ~720 h at 40 °C. In low-temperature esterification of fatty acid with aliphatic alcohols in organic solvents, the lipase activity was 5–6 times increased after inclusion of carbon nanotubes (CNT2s) and nanospheres (CNS2s) inside silica xerogel. The composite nanocarbons-in-silica biocatalysts for synthesis of isopentyl esters of capric (C10:0) and searic (C18:0) acids operated for more than 1000 h at 40 °C without loss of activity.

Author Contributions: G.A.K. conceived and designed the experiments, and wrote the paper; L.V.P. and A.B.B. performed the experiments and analyzed the experimental data; V.N. Parmon provided acquisition of the financial support for the project leading to this publication.

Acknowledgments: The authors are grateful to Sapunova L.I. and co-workers from the Institute of Microbiology (Minsk, Belarus) who provided bacteria strains producing glucose isomerase, as well as to Mamaev A.L. and all co-workers from the Institute of Biochemistry (Novosibirsk, Russia) for constructing and growing the recombinant strains-producer in order to obtain lipase-active lysates. The authors are also grateful Kuznetsov V.L. and co-workers from the Boreskov Institute of Catalysis (Novosibirsk, Russia) who produced nanocarbons and provided the CNTs, CNSs and ND for the studies. The work was conducted under the budget Project of the Boreskov Institute of Catalysis.

Conflicts of Interest: The authors declare no conflict of interest.

Abbreviations

CNT	carbon nanotube, multi-walled
CNF	carbon nanofiber
CNS	carbon nanosphere, onion-like
EAC	enzymatic active component of the heterogeneous biocatalyst
GI	glucose isomerase
INV	invertase
LIP	lipase
U	Unit of enzyme activity defined as μmol s of converted substrate per minute under the conditions described

References

1. Bommarius, A.S.; Reidel, B.R. *Biocatalysis*; WILEY-VCH Verlag GmbH & Co. KGaA: Weinheim, Germany, 2004; pp. 2–611. ISBN 3-527-30344-8.
2. Grunwald, P. *Biocatalysis*; Imperial College Press: London, UK, 2009; pp. 2–1035. ISBN 10-1-86094-744-1.
3. Buchholz, K.; Kasche, V.; Bornscheuer, U.T. *Biocatalysts and Enzyme Technology*; WILEY-VCH Verlag GmbH & Co. KGaA: Weinheim, Germany, 2005; pp. 2–431. ISBN 10-3-527-30497-5.
4. Hou, C.H. *Handbook of Industrial Biocatalysis*; Taylor & Francis Group, LLC: Abingdon, UK, 2005; pp. 2–900. ISBN 0-8247-2423-2.
5. Tao, J.; Kazlauskas, R. (Eds.) *Biocatalysis for Green Chemistry and Chemical Process Development*; WILEY, John Wiley & Sons, Inc.: Hoboken, NJ, USA, 2011; pp. 1–479. ISBN 978-0-470-43778-0.
6. Rodgers, L.E.; Holden, P.J.; Hanna, J.V.; Foster, L.J.R.; Knott, R.B.; Pike, K.J.; Bartlett, J.R. Structural evolution and stability of sol–gel biocatalysts. *Physica B* **2006**, *385–386*, 508–510. [[CrossRef](#)]
7. Illanes, A.; Wilson, L.; Vera, C. *Problem Solving in Enzyme Biocatalysis*; WILEY, John Wiley & Sons, Inc.: Hoboken, NJ, USA, 2014; pp. 141–180. ISBN 978-1-118-34171-1.
8. Kovalenko, G.A.; Sukhinin, S.V.; Perminova, L.V. Vortex Reactors for Heterogeneous Biocatalytical Processes. In *Industrial Application of Biotechnology*; Krylov, I.A., Zaikov, G.E., Eds.; NOVA Science Publisher, Inc.: New York, NY, USA, 2006; pp. 45–53.
9. Kovalenko, G.A.; Perminova, L.V. Immobilization of glucoamylase by adsorption on carbon supports and its application for heterogeneous hydrolysis of dextrin. *Carbohydr. Res.* **2008**, *343*, 1202–1211. [[CrossRef](#)] [[PubMed](#)]
10. Kovalenko, G.A.; Perminova, L.V.; Terentyeva, T.G.; Sapunova, L.I.; Lobanok, A.G.; Chuenko, T.V.; Rudina, N.A.; Cherhyak, E.I. Glucose isomerase activity in suspensions of *Arthrobacter nicotianae* cells and adsorption immobilization of the microorganisms on inorganic carriers. *Appl. Biochem. Microbiol.* **2008**, *44*, 174–181. [[CrossRef](#)]
11. Kovalenko, G.A.; Perminova, L.V.; Rudina, N.A.; Maksimova, Y.G.; Maksimov, A.Y. Saproel-based supports as novel macroporous carbon-mineral adsorbents for enzymatic active substances. *Resour. Effic. Technol.* **2016**, *2*, 159–167. [[CrossRef](#)]
12. Perminova, L.V.; Kovalenko, G.A.; Rudina, N.A.; Sapunova, L.I.; Tamkovic, I.O.; Lobanok, A.G. Catalytical properties of *Arthrobacter nicotianae* cells, a producer of glucose isomerase, immobilized inside xerogel of silicium dioxide. *Appl. Biochem. Microbiol.* **2009**, *45*, 389–394. [[CrossRef](#)]
13. Kovalenko, G.A.; Perminova, L.V.; Chernyak, E.I.; Sapunova, L.I. Investigation on macrokinetics of heterogeneous process of monosaccharide isomerization using non-growing cells of a glucose isomerase producer *Arthrobacter nicotianae* immobilized inside SiO₂-xerogel. *Appl. Biochem. Microbiol.* **2010**, *46*, 697–705. [[CrossRef](#)]
14. Kovalenko, G.A.; Perminova, L.V.; Sapunova, L.I. A peculiar method for immobilization of non-growing microbial cells by entrapment into silica xerogel. In *Biotechnology in Medicine, Foodstuffs, Biocatalysis, Environment and Biogeotechnology*; Varfolomeev, S.D., Zaikov, G.E., Krylova, L.P., Eds.; NOVA Science Publisher, Inc.: New York, NY, USA, 2010; pp. 41–49.
15. Kovalenko, G.A.; Simonova, L.G.; Perminova, L.V.; Yakushko, R.I. Biocatalyst, Method of Its Preparation and Method of Production of Glucose-Fructose Syrups. Patent RU 2341560 C1, 10 June 2008.

16. Kovalenko, G.A.; Beklemishev, A.B.; Perminova, L.V.; Mamaev, A.L.; Rudina, N.A.; Moseenkov, S.I.; Kuznetsov, V.L. Immobilization of recombinant *E. coli* thermostable lipase by entrapment inside silica xerogel and nanocarbon-in-silica composites. *J. Mol. Catal. B Enzym.* **2013**, *98*, 78–86. [\[CrossRef\]](#)
17. Kovalenko, G.A.; Perminova, L.V.; Beklemishev, A.B.; Tkachenko, V.I. Study on physicochemical properties of biocatalysts with thermostable lipase activity and final products of triglycerides' interesterification. *Appl. Biochem. Microbiol.* **2014**, *50*, 709–721. [\[CrossRef\]](#)
18. Kovalenko, G.A.; Perminova, L.V.; Rudina, N.A.; Mazov, I.N.; Moseenkov, S.I.; Kuznetsov, V.L. Immobilization of enzymatic active substances by immuring inside nanocarbon-in-silica composites. *J. Mol. Catal. B Enzym.* **2012**, *76*, 116–124. [\[CrossRef\]](#)
19. Kovalenko, G.A.; Beklemishev, A.B.; Perminova, L.V.; Chuenko, T.V.; Mamaev, A.L.; Ivanov, I.D.; Moseenkov, S.I.; Kuznetsov, V.L. Recombinant strain producing thermostable lipase from *Thermomyces lanuginosus* immobilized into nanocarbon-in-silica matrixes and properties of prepared biocatalysts. *Appl. Biochem. Microbiol.* **2013**, *49*, 296–305. [\[CrossRef\]](#)
20. Kovalenko, G.A.; Perminova, L.V.; Lenskaya, V.M.; Sapunova, L.I.; Tamkovich, I.O.; Lobanok, A.G. Biocatalyst, Method of Its Preparation and Method of Production of Glucose-Fructose Syrups. Patent Eurasia 01766 B1, 30 November 2012.
21. Kovalenko, G.A.; Perminova, L.V.; Chuenko, T.V.; Sapunova, L.I.; Shlyakhotko, E.A.; Lobanok, A.G. Immobilization of a recombinant strain producing glucose isomerase inside SiO₂-xerogel and properties of prepared biocatalysts. *Appl. Biochem. Microbiol.* **2011**, *47*, 151–157. [\[CrossRef\]](#)
22. D'Souza, S.F.; Melo, J.S. Immobilization of bakers yeast on jute fabric through adhesion using polyethyleneimine: Application in an annular column reactor for the inversion of sucrose. *Process. Biochem.* **2001**, *36*, 677–681. [\[CrossRef\]](#)
23. Sungur, S.; Al-Taweel, R.; Yildirim, O.; Logoglu, E. Immobilization of *Saccharomyces cerevisiae* in gelatin cross-linked with chromium ions for conversion of sucrose by intracellular invertase. *Polym. Plast. Technol. Eng.* **2006**, *45*, 929–934. [\[CrossRef\]](#)
24. Hasal, P.; Vojtisek, V.; Lejkova, A.; Kleczek, P.; Kofronova, O. An immobilized whole yeast cell biocatalyst for enzymatic sucrose hydrolysis. *Enzym. Microb. Technol.* **1992**, *14*, 221–229. [\[CrossRef\]](#)
25. Nassif, N.; Bouvet, O.; Rager, M.N.; Roux, C.; Coradin, T.; Livage, J. Living bacteria in silica gels. *Nat. Mater.* **2002**, *1*, 42–44. [\[CrossRef\]](#) [\[PubMed\]](#)
26. Carturan, G.; Campostrini, R.; Dir, S.; Scardi, V.; De Alteriis, E. Inorganic gels for immobilization of biocatalysts: Inclusion of invertase-active whole cells of yeast (*Saccharomyces cerevisiae*) into thin layers of SiO₂ gel deposited on glass sheets. *J. Mol. Catal.* **1989**, *57*, L13–L16. [\[CrossRef\]](#)
27. Kovalenko, G.A.; Perminova, L.V. Biocatalyst, Method of Its Preparation and Method of Production of Invert Syrup Using This Biocatalyst. Patent RU 2372403 C1, 10 November 2009.
28. Kovalenko, G.A.; Perminova, L.V.; Plaksin, G.V.; Komova, O.V.; Chuenko, T.V.; Rudina, N.A. Immobilized yeast membranes as biocatalysts for sucrose inversion. *Appl. Biochem. Microbiol.* **2005**, *41*, 399–403. [\[CrossRef\]](#)
29. Mateo, C.; Palomo, J.M.; Lorente, G.; Guisan, J.M.; Fernandez-Lafuente, R. Improvement of enzyme activity, stability and selectivity via immobilization techniques. *Enzym. Microb. Technol.* **2007**, *40*, 1451–1463. [\[CrossRef\]](#)
30. Rodrigues, R.C.; Fernandez-Lafuente, R. Lipase from *Rhizomucor miehei* as an industrial biocatalyst in chemical process. *J. Mol. Catal. B Enzym.* **2010**, *64*, 1–22. [\[CrossRef\]](#)
31. Rodrigues, R.C.; Fernandez-Lafuente, R. Lipase from *Rhizomucor miehei* as a biocatalyst in fats and oils modification. *J. Mol. Catal. B Enzym.* **2010**, *66*, 15–32. [\[CrossRef\]](#)
32. Contesini, F.J.; Lopes, D.B.; Macedo, G.A.; da G. Nascimento, M.; de O. Carvalho, P. *Aspergillus* sp. lipase: Potential biocatalyst for industrial use. *J. Mol. Catal. B Enzym.* **2010**, *67*, 163–171. [\[CrossRef\]](#)
33. Fernandez-Lafuente, R. Lipase from *Thermomyces lanuginosus*: Uses and prospects as an industrial biocatalyst. *J. Mol. Catal. B Enzym.* **2010**, *62*, 197–212. [\[CrossRef\]](#)
34. Itabaiana, I., Jr.; Miranda, L.S.M.; Mendon, R.O.; de Souza, R.O.M.A. Towards a continuous flow environment for lipase-catalyzed reactions. *J. Mol. Catal. B Enzym.* **2013**, *85–86*, 1–9. [\[CrossRef\]](#)
35. Bezborodov, A.M.; Zagustina, N.A. Lipases in catalytic reactions of organic synthesis (review). *Appl. Biochem. Microbiol.* **2014**, *50*, 313–337. [\[CrossRef\]](#)
36. Perminova, L.V.; Kovalenko, G.A.; Beklemishev, A.B.; Mamaev, A.L.; Pykhtina, M.B.; Rudina, N.A. Catalytic properties of lipase entrapped as lysates of recombinant strain-producer *rEscherichia coli*/lip into

- nanocarbon-in-silica composites in the bioconversion of triglycerides and fatty acids. *Appl. Biochem. Microbiol.* **2018**, *54*, 38–44. [[CrossRef](#)]
37. Sokolovskii, V.D.; Kovalenko, G.A. Immobilization of oxydoreductases on inorganic supports based on alumina: The role of mutual correspondence of enzyme-support hydrophobic-hydrophilic characters. *Biotechnol. Bioeng.* **1988**, *32*, 916–919. [[CrossRef](#)] [[PubMed](#)]
 38. Kovalenko, G.A.; Sokolovskii, V.D. Immobilization of oxydoreductases on inorganic supports based on alumina: Immobilization of alcohol dehydrogenase on nonmodified and modified alumina. *Biotechnol. Bioeng.* **1983**, *25*, 3177–3184. [[CrossRef](#)] [[PubMed](#)]
 39. Kovalenko, G.A.; Perminova, L.V.; Chuenko, T.V.; Rudina, N.A. Tuning surface morphology of inorganic supports for adsorptive immobilization of enzymatic active substances. *Compos. Interfaces* **2009**, *16*, 293–305. [[CrossRef](#)]
 40. Kovalenko, G.A.; Beklemishev, A.B.; Perminova, L.V.; Mamaev, A.L.; Chuenko, T.V.; Kuznetsov, V.L. Biocatalyst, Method of Its Preparation and Method of Interesterification of Vegetable Oils Using This Biocatalyst. Patent RU 2539101 C2, 10 January 2014.
 41. Kovalenko, G.A.; Perminova, L.V.; Beklemishev, A.B.; Yakovleva, E.Y.; Pykhtina, M.B. Heterogeneous biocatalytic processes of vegetable oil interesterification to biodiesel. *Catal. Ind.* **2015**, *7*, 73–81. [[CrossRef](#)]
 42. Kovalenko, G.A.; Perminova, L.V.; Beklemishev, A.B.; Mamaev, A.L.; Patrushev, Y.V. Heterogeneous biocatalytic processes of esterification of saturated fatty acids with aliphatic alcohols. *Catal. Ind.* **2018**, *10*, 68–74. [[CrossRef](#)]
 43. Perminova, L.V.; Kovalenko, G.A.; Chukanov, N.V.; Patrushev, Y.V. Enzymatic esterification of saturated fatty acids with aliphatic alcohols as an alternative method of a low-temperature synthesis of esters. *Russ. Chem. Bull.* **2017**, *66*, 1–4. [[CrossRef](#)]
 44. Joseph, M.D.; Kasprzak, D.J.; Crouch, S.R. A stopped-flow clinical analyzer in which immobilized-enzyme reaction loops are used. *Clin. Chem.* **1977**, *23*, 1033–1036. [[PubMed](#)]
 45. Usoltseva, A.N.; Kuznetsov, V.L.; Rudina, N.A.; Moroz, E.M.; Haluska, M.; Roth, S. Influence of catalysts activation on their activity and selectivity in carbon nanotubes synthesis. *Phys. Status Solidi* **2007**, *244*, 3920–3924. [[CrossRef](#)]
 46. Kuznetsov, V.L.; Chuvilin, A.L.; Moroz, E.M.; Kolomiichuk, V.N.; Shaichutdinov, S.K.; Butenko, Y.V.; Malkov, I.Y. Effect of explosion conditions on the structure of detonation soot: Ultra disperse diamond and onion carbon. *Carbon* **1994**, *32*, 873–882. [[CrossRef](#)]
 47. Kuznetsov, V.L.; Chuvilin, A.L.; Butenko, Y.V.; Malkov, I.Y.; Titov, V.M. Onion-like carbon from ultra disperse diamond. *Chem. Phys. Lett.* **1994**, *222*, 343–348. [[CrossRef](#)]

48. Kuvshinov, G.G.; Mogilnykh, Y.I.; Kuvshinov, D.G.; Zaikovskii, V.I.; Avdeeva, L.B. Peculiarities of filamentous carbon formation in methane decomposition in Ni-containing catalysts. *Carbon* **1998**, *36*, 87–97. [[CrossRef](#)]
49. Kuvshinov, G.G.; Mogilnykh, Y.I.; Kuvshinov, D.G. Kinetics of carbon formation from CH₄-H₂ mixtures over a nickel containing catalyst. *Catal. Today*. **1998**, *42*, 357–360. [[CrossRef](#)]



© 2018 by the authors. Licensee MDPI, Basel, Switzerland. This article is an open access article distributed under the terms and conditions of the Creative Commons Attribution (CC BY) license (<http://creativecommons.org/licenses/by/4.0/>).